Polymer 50 (2009) 3981–3989

Contents lists available at ScienceDirect

Polymer

journal homepage: www.elsevier.com/locate/polymer

Structure and properties of MDO stretched polypropylene

Seyed H. Tabatabaei, Pierre J. Carreau*, Abdellah Ajji

CREPEC, Chemical Engineering Department, Ecole Polytechnique, C.P. 6079, Succ. Centre ville, Montreal, QC, H3C 3A7 Canada

ARTICLE INFO

Article history:
Received 24 April 2009
Received in revised form
9 June 2009
Accepted 11 June 2009
Available online 30 June 2009

Keywords:
Polypropylene
MDO process
Hot drawing

ABSTRACT

Two polypropylene cast films of different crystalline structures (one with coexisting small rows of lamellae and spherulites and the other with only a spherulitic structure) were prepared by extrusion. The produced cast films were uniaxially hot drawn at $T = 120\ ^{\circ}C$ using a machine direction orientation (MDO) unit and the changes in structure and morphology were examined and related to barrier as well as tear and puncture properties. Structural changes in terms of the degree of crystallinity and crystal size distribution, orientation of the amorphous and crystalline phases, and the deformation behavior at the crystal lattice and lamellae scales were investigated using differential scanning calorimetry (DSC), Fourier transform infrared spectroscopy (FTIR), wide angle X-ray diffraction (WAXD), and small angle X-ray scattering (SAXS), respectively. A significant effect of the original crystal morphology on the alignment of the amorphous and crystalline phases was observed from FTIR and WAXD. The results also revealed that the deformation behavior of the crystal structure was dependent on the draw ratio (DR). Our findings showed that by increasing DR the crystal lamellae first broke up and oriented along the drawing direction and then, at large DR, they were deformed and created a fibrillar structure. Morphological pictograms illustrating the effects of original morphology and draw ratio on the stretched film microstructure are proposed. The tear resistance along the machine direction (MD) decreased significantly with increasing DR whereas the puncture resistance increased drastically. Finally, the oxygen transmission rate (OTR) of the MDO stretched films could be correlated with the orientation parameters as well as the β-relaxation peak magnitude of the amorphous tie chains.

1. Introduction

Polypropylene is one of the most widely used polymers for the production of plastic films. Applications cover packaging to microporous membranes. There are two main industrial processes for the production of PP films: film blowing and cast film extrusion followed by stretching (above and below the melt temperature). Although the films obtained from both processes could have the same thicknesses, their properties such as mechanical and clarity could be quite different as a result of the differences in the process conditions.

It is well known that uniaxial or biaxial drawing of the polymeric films such as polypropylene, polyester, polyketone, nylon, and ethyl vinyl alcohol can drastically affect their properties, particularly mechanical, impact, barrier, and optical properties [1–7].

The machine direction orientation (MDO) process is widely used for uniaxial stretching of polyethylene and polypropylene films. The MDO unit can be operated either in-line or off-line with extrusion and is controlled via variables such as: the distance between the draw rollers, draw ratio, drawing speed, drawing times (a film can be stretched many times), drawing temperature, and heat-setting conditions [1]. The stretching is usually performed at a high temperature, below the melt temperature of the polymer, and results in a highly oriented film that causes anisotropy in properties. The drawing process usually improves the strength and barrier properties, but brings some drawbacks such as a reduction of the tear resistance along the machine direction (MD) and a lowering of elongation at break along the transverse direction (TD) [1]. For example, Schut [2] used the MDO process to improve the barrier properties of nylon and ethyl vinyl alcohol, but the films were brittle and had low tear resistance in MD.

The stretching of a well oriented shish-kebab crystal morphology involves the separation of the stacked lamellae, leading to pores formation and subsequent microporous membrane generation [8,9]. However, the drawing of polypropylene films possessing spherulitic crystal structure involves a morphological transformation of the spherulites, which will affect their final properties.

The evolution of the crystal structure of biaxial as well as uniaxial drawn films has been investigated in the literature [10–13]. Nie et al. [10] studied the morphological development during biaxial stretching of polypropylene films using atomic force microscopy (AFM). According to their results, the biaxial orientation of polypropylene involved a morphological transformation of the spherulites into

* Corresponding author. Tel.: +1 514 340 4711x4924; fax: +1 514 340 2994.
E-mail address: pcarreau@polymtl.ca (P.J. Carreau).

0032-3861/$ – see front matter © 2009 Elsevier Ltd. All rights reserved.
doi:10.1016/j.polymer.2009.06.059

a network of microfibrils, which was also confirmed by Diez et al. [11]. Sadeghi et al. [1] studied the morphology development during MDO stretching of PP. Their results showed a fibrillar crystalline structure at a high draw ratio (DR), such as DR = 6. Also, a distinctive improvement in the mechanical, clarity, and barrier properties was reported as DR increased. Using in-situ small angle X-ray scattering (SAXS) and wide angle X-ray diffraction (WAXD), Zuo et al. [12] investigated the structure of polypropylene films during uniaxial stretching for various temperatures. The rate of crystal alignment during deformation at high temperatures was found to be slower than that at low temperature, but the final orientation during deformation at high temperatures was higher due to the larger applied strain. Sakurai et al. [13] investigated the structural deformation behavior of polypropylene resins of different molecular weight (Mw), molecular weight distribution (MWD), and isotacticity (IT) during hot drawing. Significant effects of Mw, MWD, and IT on the mechanical properties, morphology as well as stress distribution in the hot stretched samples were observed.

Although few authors have investigated the relationship between biaxial orientation and particularly barrier properties of various resins, very little has been reported on uniaxial drawing involving industrial scale capabilities. In this study, precursor films with a spherulitic structure and coexisting small rows of lamellae and spherulites were produced and MDO oriented using an industrial scale production line. A detailed investigation of the structure evolution with stretching has been carried out and relationships between morphological transformation and barrier, tear, and puncture properties are discussed.

2. Experimental

2.1. Material

A commercial linear polypropylene (PP5341) supplied by ExxonMobil and having a melt flow rate (MFR) of 0.8 g/10 min (under ASTM D1238 conditions of 230 °C and 2.16 kg) was selected. Its molecular weight was estimated from the relationship between the zero-shear viscosity and molecular weight [14] and found to be around 772 kg/mol. The resin showed a polydispersity index (PDI) of 2.7, as measured using a GPC (Viscotek model 350) with 1,2,4-trichlorobenzene (TCB) as a solvent and column temperature of 140 °C. Its melting point, T_m, and crystallization temperature, T_c, obtained from differential scanning calorimetry at a rate of 10 °C/min, were 161 °C and 118 °C, respectively.

2.2. Film preparation

The cast films were prepared using an industrial multilayer cast film from Davis Standard Company (Pawcatuck, CT) equipped with a 122 cm width slit die and two cooling drums. The extrusion was carried out at 220 °C and the distance between the die exit to the nip roll was 15 cm. Two precursor films of different microstructures were produced. (1) Coexisting rows of lamellae and spherulites: this morphology could be obtained when the cast roll was set at a high temperature (e.g. 120 °C) and the polymer melt at the die exit was subjected to a high draw ratio (e.g. 30). (2) Only spherulitic structure: this structure could be produced when the cast roll was set at a low temperature (e.g. 40 °C) and the film at the die was subjected to a low draw ratio (e.g. 3). Additional details regarding the process conditions could be found elsewhere [15]. In this paper, these precursor films are denoted as P-1 and P-2, respectively. Fig. 1 represents SEM surface images of the etched P-1 precursor film reported in [15]. We observe that both rows of lamellae and spherulites are present in this precursor film. To get the same final thickness of 150 μm for P-1 and P-2, the die gap was set at 4.5 and 0.45 mm, respectively.

In the MDO unit, the produced films were uniaxially stretched at 120 °C and under draw ratios ranging from 1 to 7.2. Stretching at draw ratios above 7.2 resulted in film breakage. After MDO, the films were cooled to room temperature in contact with ambient air.

2.3. Film characterization

2.3.1. Thermal analysis

The thermal properties of specimens were analyzed using differential scanning calorimetry (DSC) Q 1000 from TA Instruments. The thermal behavior of the films was obtained by heating from 50 to 220 °C at a rate of 10 °C/min. The reported crystallinity results were calculated using a heat of fusion of 209 J/g for a fully crystalline polypropylene (PP) [16].

2.3.2. Fourier transform infrared spectroscopy (FTIR)

For FTIR measurements, a Nicolet Magna 860 FTIR instrument from Thermo Electron Corp. (DTGS detector, resolution 2 cm^{-1}, accumulation of 128 scans) was used. The beam was polarized by means of a Spectra-Tech zinc selenide wire grid polarizer from Thermo Electron Corp. The measurement is based on the absorption of infrared light at certain frequencies corresponding to the vibration modes of atomic groups present within the molecule. In addition, if a specific vibration is attributed to a specific phase, the orientation within that phase can be determined [17]. If the films are oriented, the absorption of plane-polarized radiation by a vibration in two orthogonal directions, specifically parallel and perpendicular to a reference axis (MD), should be different. The ratio of these two absorption values is defined as the dichroic ratio, D [17]:

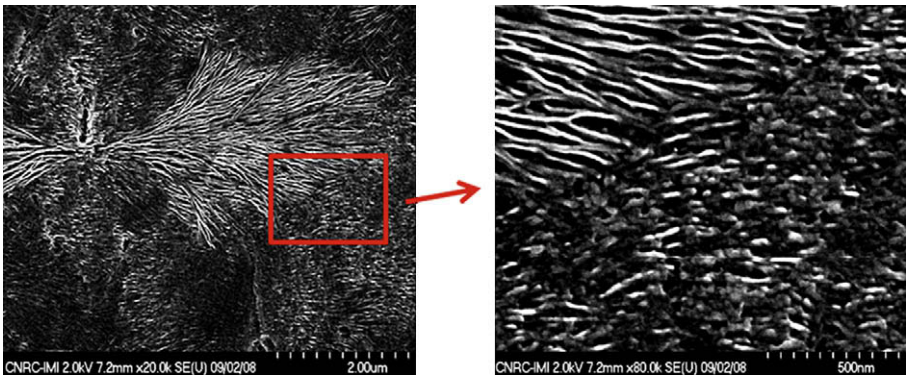

Fig. 1. SEM micrographs of the surface of the P-1 precursor film [15]. The right image is a high magnification micrograph of the section corresponding to the rectangle. MD ↑ and TD →.

$$D = \frac{A_{\parallel}}{A_{\perp}} \quad (1)$$

where $A_{\parallel}$ is the absorption parallel and $A_{\perp}$ is the absorption perpendicular to a specific reference axis. The Herman orientation function of this vibration is obtained according to [17]:

$$F = \frac{2}{3\cos^2\alpha - 1} \cdot \frac{D-1}{D+2} \quad (2)$$

where α is the angle that the transition moment makes with the polymer chain axis, which was taken equal to 18° as mentioned in Ref. [18].

For polypropylene, absorption at the wavenumber of 998 cm^{-1} is attributed to the crystalline phase (*c*-axis) while absorption at the wavenumber of 972 cm^{-1} is due to the contribution of both crystalline and amorphous phases. From the former absorption, the orientation of the crystalline phase, F_c, can be determined while from the latter, the average orientation function, F_{avg}, is obtained. The orientation of the amorphous phase, F_a, can be calculated according to:

$$F_{avg} = X_c F_c + (1 - X_c) F_a \quad (3)$$

where X_c is the degree of crystallinity. Using FTIR, the global, crystalline and amorphous orientations can be determined.

2.3.3. X-ray diffraction

XRD measurements were carried out using a Bruker AXS X-ray goniometer equipped with a Hi-STAR two-dimensional area detector. The generator was set up at 40 kV and 40 mA and the copper Cu Kα radiation ($\lambda = 1.542$ Å) was selected using a graphite crystal monochromator. The sample to detector distance was fixed at 9.2 cm for wide angle X-ray diffraction and 28.2 cm for small angle X-ray scattering analysis. To get the maximum diffraction intensity, several film layers were stacked together to obtain a total thickness of about 2 mm.

Wide angle X-ray diffraction (WAXD) is based on the diffraction of a monochromatic X-ray beam by the crystallographic planes (*hkl*) of the polymer crystalline phase. Using a pole figure accessory, the intensity of the diffracted radiation for a given *hkl* plane is measured as the sample is rotated through all possible spherical angles with respect to the beam. This gives the probability distribution of the orientation of the normal to *hkl* plane with respect to the directions of the sample.

The Herman orientation function of a crystalline axis is given by [19]:

$$F = \frac{(3 < \cos^2\phi > -1)}{2} \quad (4)$$

where ϕ is the angle between the unit cell axes (*a*, *b*, and *c*) and reference axes. Details about the calculations can be found elsewhere [19].

The orientation factors from WAXD are mainly due to the crystalline part, therefore no information about the orientation of the amorphous phase can be obtained. Small angle X-ray scattering (SAXS) was used to compare the level of lamellae formation for the different samples.

2.3.4. Puncture and tear analysis

Puncture tests were performed using a 10 N load cell of an Instron 5500R machine. A needle with 0.5 mm radius was used to pierce the samples. The film was held tight in the camping device with a central hole of 11.3 mm. The displacement of the film was recorded against the force (N) and the maximum force was reported as the puncture strength.

A standard test method for the tear resistance of plastic films based on ASTM D1922 was used to obtain MD and TD tear resistances. According to this standard, the work required in tearing is measured by the loss of energy of an encoder, which records the angular position of the pendulum during the tearing operation.

2.3.5. Oxygen transmission

Oxygen transmission rates (OTRs) were determined using a modification of the ASTM Standard Method D 3985-81 with an Ox-Tran Model 2/21 apparatus (Mocon Inc., Minneapolis, MN) at 25 °C. In this paper, all OTR values presented have been normalized (multiplied) by the films thickness. Two films of each specimen were tested and the average value is reported.

2.3.6. Dynamic mechanical thermal analysis (DMTA)

Dynamic thermomechanical properties of different samples were characterized using a dynamic mechanical thermal analyzer (DMTA) 2980 from TA Instruments, inside an environmental test chamber (ETC). Specimens cut parallel to the drawing direction were subjected to a dynamic tensile deformation mode. The temperature ranged from −60 °C to 120 °C at a rate of 2 °C/min and a frequency of 1 Hz was applied to the rectangular samples. To generate low temperatures and to control temperature during heating, liquid nitrogen was used. The β-relaxation was determined from the peak magnitude of the tan δ curves.

3. Results and discussion

We first present experimental data that clearly demonstrate the effect of draw ratio (DR) and initial crystal morphology on the degree of crystallinity and crystal size distribution, orientation of the amorphous and crystalline phases, deformation behavior at the crystal lattice and lamellae scales. Subsequently, morphological pictograms, illustrating the influence of DR and original morphology on the final structure of the drawn films are proposed. Finally, puncture resistance along the normal direction (ND), tear data along the machine direction (MD), and oxygen transmission rate (OTR) results are presented and their correlations with the structural parameters such as orientation function are reported and discussed.

The effect of draw ratio on the thermal behavior of the films for P-1 is shown in Fig. 2. The thermogram of the film before drawing (DR = 1) exhibits a main melting peak at 158 °C and a small peak at 144 °C. The small peak at 144 °C suggests the presence of a bimodal crystal size distribution (the WAXD measurements for this specimen showed no intensity peaks corresponding to the beta crystal form. Therefore, the presence of this type of crystal is excluded). No peak around 144 °C was observed for the unstretched P-2 sample (not shown), indicating the presence of more uniform crystal sizes. As seen in Fig. 2, increasing DR shifts the melting peak, $T_{m,max}$, to much higher values and a shoulder at the same temperature as the melting peak of the unstretched film appears, suggesting again the presence of crystals of different sizes. The shoulder is related to spherulites and/or rows of lamellae that were not or slightly deformed whereas the peak at the higher temperature is due to the formation of fibrils following the deformation, consistent with the SAXS results that will be discussed later. A double melting point for the specific shish-kebab structure of a polypropylene (PP) has also been observed by Somani et al. [20]. According to them, the shish in PP had a melting temperature of about 5–10 °C higher than that of the kebabs and about 15–20 °C higher than that for spherulites. Elias et al. [21] reported also a double melting peak for a PP drawn by 5.5 times. They attributed their results to a connectivity of the chains in the shish or fibrils that resulted in a large crystal thickness and, as a consequence, a higher melting point than in the case of the spherulites. In our case, it is believed that by increasing DR, a fibrillar structure is formed,

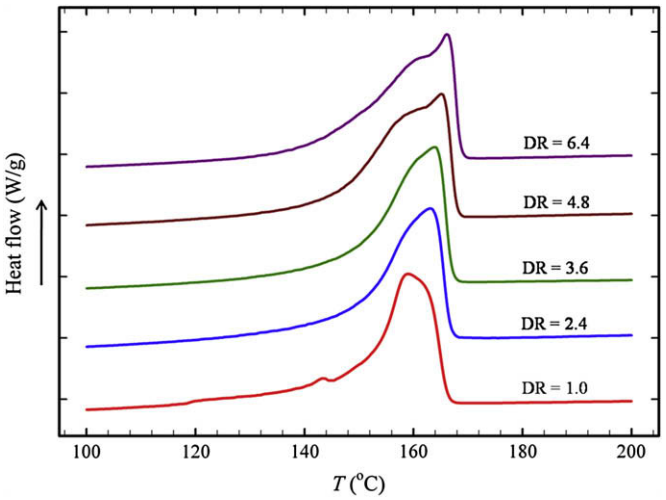

Fig. 2. DSC heating thermograms for P-1 films obtained under different draw ratios.

leading to a thicker crystal structure and consequently a higher $T_{m,max}$. The DR dependence of the degree of crystallinity (X_c) of the samples was also evaluated using DSC (not shown). The films obtained from P-1 showed crystallinity around 10% larger than those prepared from P-2. In addition, increasing DR up to 7.2 enhanced the crystallinity by about 10% for both P-1 and P-2.

The orientation and arrangement of the phases (either crystalline or amorphous) in polypropylene films are key factors in controlling their final properties. Figs. 3 and 4 present the Herman orientation functions of the crystalline phase, F_c, as well as of the amorphous phase, F_a, obtained from FTIR, respectively. The orientation parameters before stretching (DR = 1) are quite low, because of the presence of spherulites. However, as expected increasing DR drastically increases F_c and F_a (Figs. 3 and 4, respectively). Furthermore, the rate of increase of the orientation functions for DR between 1 and 3.2 is much larger than beyond DR = 3.2, indicating a stronger crystal alignment at the initial stages of deformation. It is postulated that at low DR, break up and tilting of the spherulites and/or rows of lamellae occur whereas at high deformations the tilted crystals are stretched and form fibrillar structure along the machine direction (MD). Due to the presence of small rows of lamellae crystals in P-1 films, they show larger crystalline and amorphous orientation functions below DR = 1.6 (Figs. 3 and 4, respectively). However, at DR between 1.6 and 3.2, drawn P-2 films

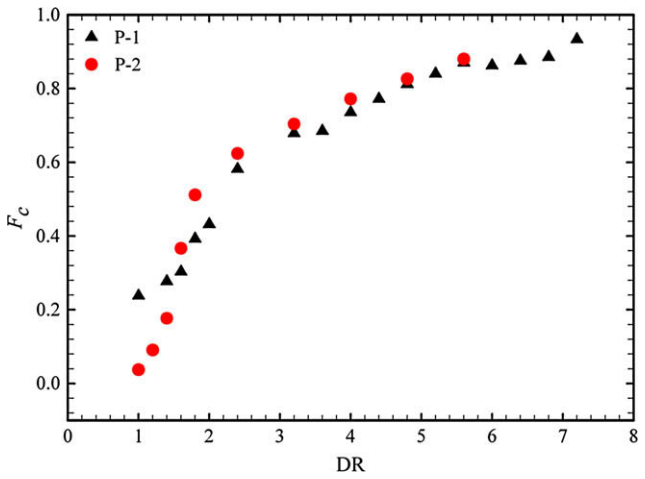

Fig. 3. Crystalline orientation function as a function of draw ratio.

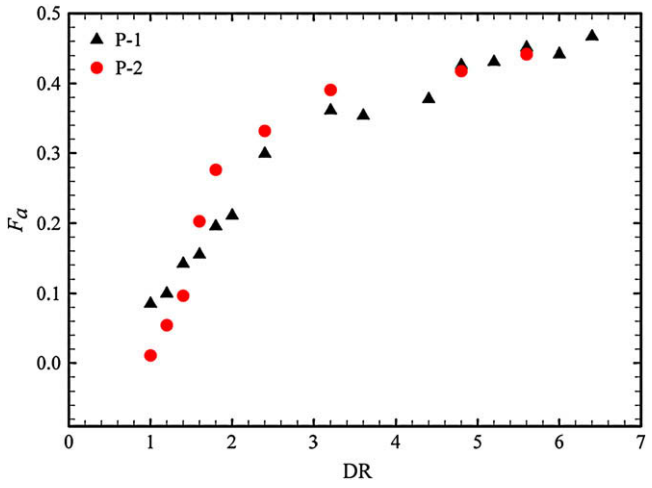

Fig. 4. Amorphous orientation function as a function of draw ratio.

show better alignment compared with those of P-1. This was also confirmed by wide angle X-ray diffraction (WAXD) and this behavior will be discussed later. Furthermore, at over DR = 3.2, P-1 and P-2 films show almost identical orientation values, indicating somewhat similar microstructures.

The effect of draw ratio on orientation of the crystalline phase using WAXD is shown in Fig. 5. In the WAXD patterns, the first and second rings represent the 110 and 040 crystalline reflections,

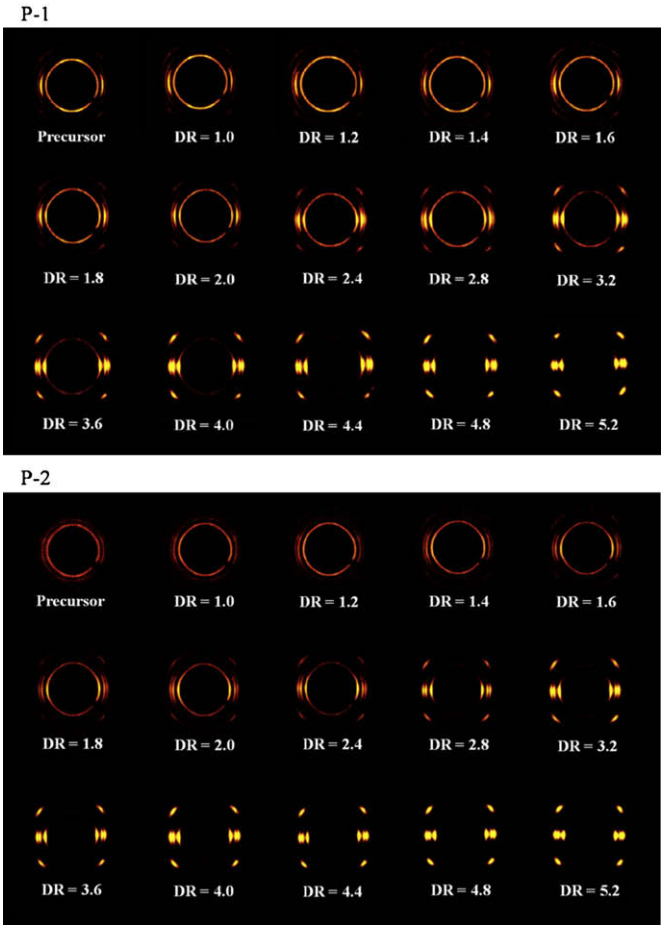

Fig. 5. 2D WAXD patterns for P-1 (top) and P-2 (bottom) films obtained under different draw ratios.

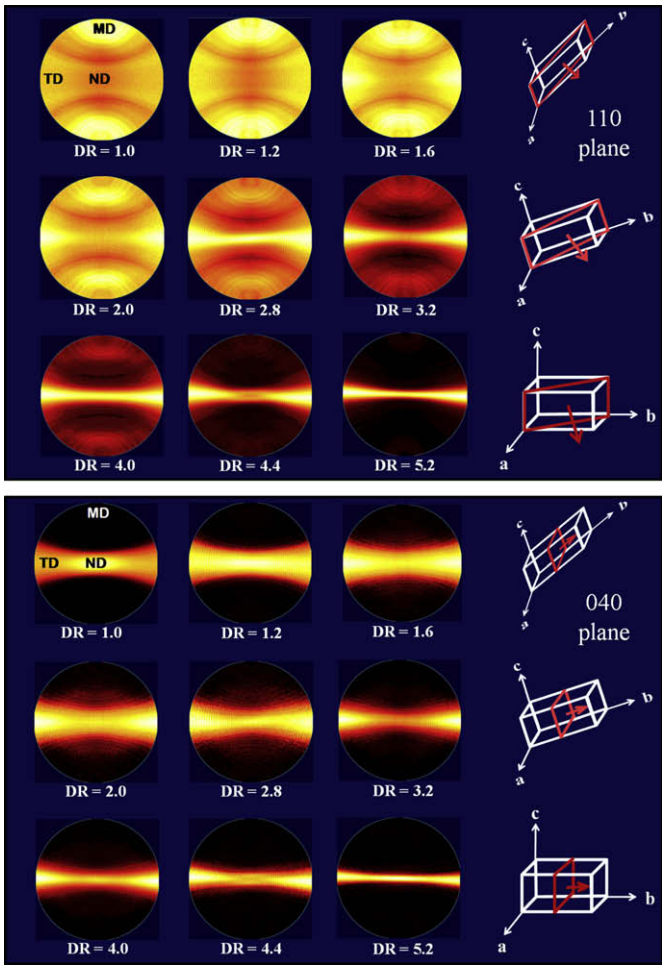

Fig. 6. Pole figures of 110 (top) and 040 (bottom) reflections for P-1 films obtained under different draw ratios.

respectively [19]. At low draw ratios, a diffraction ring is seen for the 110 crystallographic plane for P-1 and P-2, indicating low crystalline phase orientation. However, by increasing DR, the diffraction intensity along the meridian decreases gradually and disappears beyond DR = 4.0 and 2.4 for P-1 and P-2, respectively. In contrast, the diffraction intensity in the equator increases drastically when DR increases up to 4, while further increases of DR has a slight impact on the WAXD pattern. As expected, compared with precursor films with coexisting rows of lamellae and spherulites (P-1), the only spherulitic structure (P-2) film reveals a ring shape diffraction with less intensities at low DR (e.g. DR = 1.2), implying much lower orientation for P-2. However, at medium draw ratios (e.g. DR = 2.8), the diffraction pattern for P-2 demonstrates only arcs that are sharper and more concentrated in the center, indicating more orientation compared to P-1. Due to the larger size of the spherulites compared to the small rows of lamellae (see Fig. 1), spherulites in PP are expected to deform more easily than rows of lamellae. This is possibly why at medium DR, the P-2 samples exhibit a better crystal orientation. In other words, at medium DR, the P-1 films contain some initial rows of lamellae that might not have been completely tilted. At very large DR, no remarkable differences among the WAXD patterns of P-1 and P-2 can be recognized, suggesting that the main structural transformations occur below DR = 4.4.

The crystalline orientation can also be analyzed quantitatively from the pole figures of the 110 and 040 planes and the results for P-1 are illustrated in Fig. 6. The schematics in the figure represent

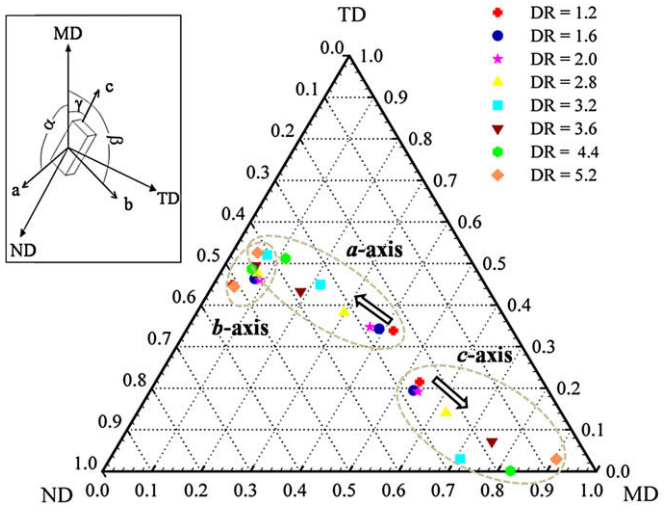

Fig. 7. Orientation characteristics as $\cos^2(\phi)$ of the crystal axes (a, b, and c) along MD, TD, and ND for P-1 (the arrows represent the shift of $\cos^2(\phi)$ with increasing DR).

the crystal alignment based on their pole figures at low, medium, and high stretch ratios. The normal to the 110 plane is the bisector of the a and b axes and 040 is along the b-axis of crystal unit cells [19]. Before drawing (DR = 1), slight orientations of the 110 and 040 planes are detected in MD and ND, respectively. Increasing DR causes the orientation of the 110 plane along MD gradually to

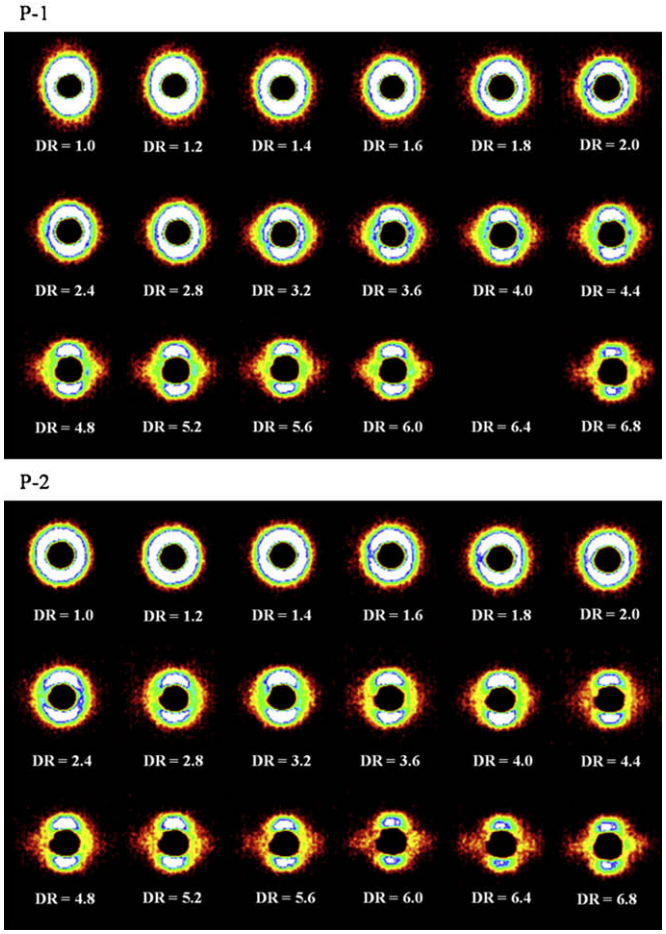

Fig. 8. 2D SAXS patterns for P-1 (top) and P-2 (bottom) films obtained under different draw ratios.

decrease until it vanishes at large DR. However, this crystallographic plane first moves into TD and then to both TD and ND at large DR. It is clear that the 040 plane (*b*-axis) was initially oriented along ND and upon drawing appreciably moves into TD.

The orientation features, in terms of $\cos^2(\phi)$ of the crystalline axes (i.e. *a*, *b*, and *c* (see the sketch in Fig. 7)) along MD, TD, and ND obtained from the Herman orientation function for stretched films of P-1 are plotted in the triangular diagram of Fig. 7. It is obvious that increasing DR yields a large movement of the *c*-axis of the crystals towards MD (the *c*-axis orientation feature varies from 0.5 to 0.9 as DR changes from 1 to 5.2). Furthermore, increasing DR causes the *a*-axis of the crystals to take a position closer to the TD and ND planes whereas the *b*-axis, for all DR, remains close to the TD and ND planes. These clearly elucidate the significant improvement in orientation by increasing DR, in accordance with the FTIR data presented in Fig. 3. However, it should be mentioned that the orientation functions obtained using FTIR were slightly larger than the ones from the WAXD pole figures. These discrepancies in the values of the measured *c*-axis orientation may be due to different factors such as peak deconvolution, contribution of the amorphous phase, etc. as discussed for PE and PP elsewhere [22,23].

SAXS measurements show in Fig. 8 the effects of draw ratio as well as initial morphology on lamellae deformation. The meridian streak in the SAXS pattern is attributed to the lamellae perpendicular to the machine direction (MD), while the equatorial maxima are attributed to the lamellae perpendicular to the transverse direction (TD) and/or the fibrils aligned into MD. Before drawing (DR = 1), due to the presence of spherulites or random lamellae nearby circular patterns for P-1 as well as P-2 are observed. The more intense streak in the meridian for the precursor (DR = 1) of P-1 is related to the presence of rows of lamellae that has been formed somewhat perpendicular to MD. Due to the lamellae deformation, the meridian streak monotonically decreases as DR increases, but does not disappear even at large DR. This suggests the presence of some lamellae perpendicular to MD even at large DR. However, the equatorial streak decreases as draw ratio increases up to 4.0 and 2.4

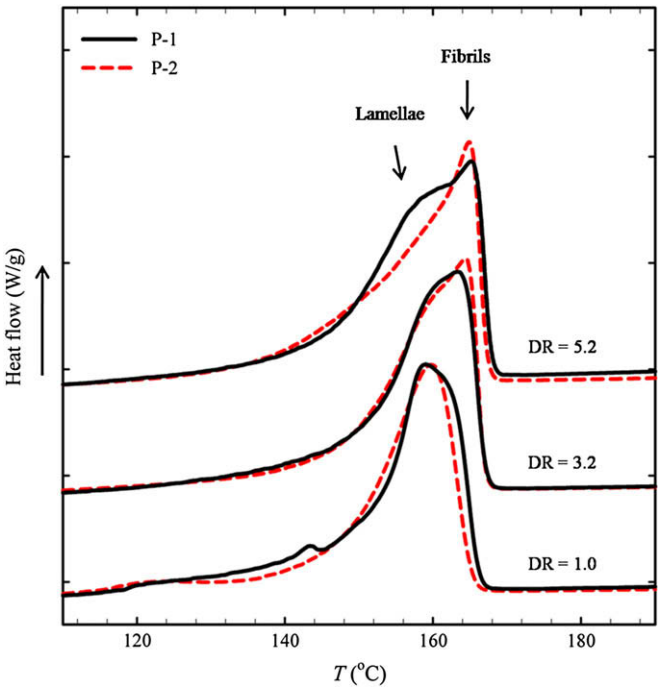

Fig. 9. DSC heating thermograms for P-1 and P-2 films obtained under draw ratios of 1.0, 3.2, and 5.2.

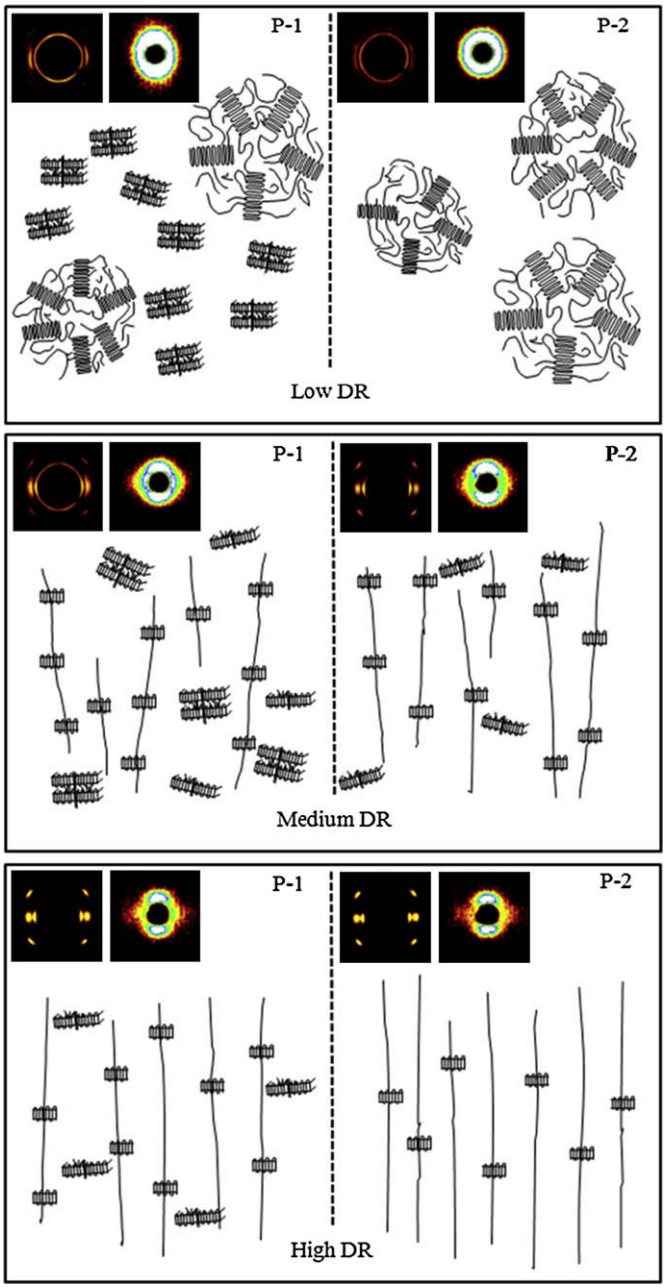

Fig. 10. Proposed pictograms of the molecular structure for P-1 and P-2 films obtained under low, medium, and high draw ratios.

for P-1 and P-2, respectively, suggesting again more crystal deformation for P-2 compared to P-1. Further increase of DR causes the equatorial intensity to slightly increase. In fact, drawing of the PP films causes the break up and tilting of the crystal lamellae in the spherulites and the formation of fibrillar structure along MD. On the one hand, the deformation of the lamellae in the spherulites reduces the equatorial intensity, on the other hand fibrils are created leading to an increase in the equatorial intensity. However, it should be mentioned that our SAXS instrument was not very sensitive to the detection of fibrils in the equator. Therefore, in Fig. 9, we reconsider the DSC data to qualitatively compare the amount of lamellae and/or fibrils in P-1 and P-2 for various DR. Before drawing (DR = 1), no significant differences between the melting curve of P-1 and P-2 are observed. However, at DR = 3.2, the thermograms of P-1 and P-2 exhibit a peak as well as a small shoulder at temperatures of 163 °C

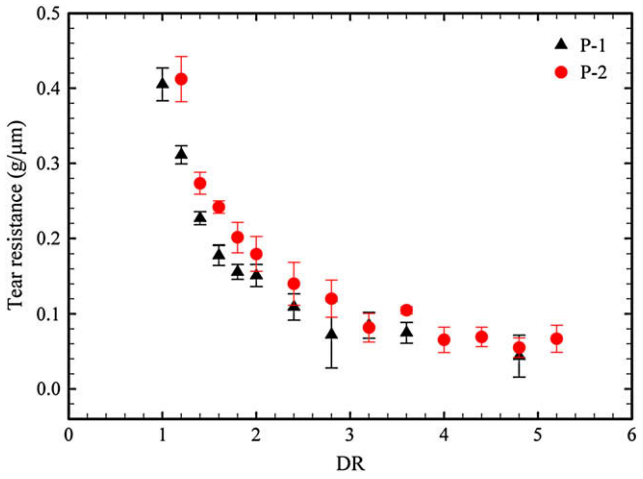

Fig. 11. Tear resistance along MD as a function of draw ratio for P-1 and P-2.

and 158 °C, respectively. As mentioned earlier, the peak and shoulder are attributed to the presence of fibrils and lamellae, respectively. Clearly, the contribution of fibrils to the crystals in P-2 is more important than in P-1. At DR = 5.2, the shoulder for P-2 becomes very small whereas P-1 shows a large shoulder, which again suggests the presence of more fibrils in the stretched P-2 film.

Based on our observations from thermal analysis, FTIR results, WAXD and SAXS patterns, microstructural pictograms illustrating the effects of draw ratio and original morphology on the crystallite arrangements are proposed in Fig. 10. At low draw ratios, FTIR data, WAXD and SAXS patterns suggested a crystal structure with coexisting rows of lamellae and spherulites for the P-1 films and only spherulites for P-2, respectively. At medium DR, the SAXS data revealed that a major part of the crystal lamellae are broken up and tilted to form fibrils. The coexisting lamellae and fibrils for the stretched samples were also confirmed by DSC results (see Figs. 2 and 9). However, WAXD and FTIR analyses indicated that P-2, at medium DR, showed higher orientation than P-1 and also the SAXS patterns showed a better crystallite deformation and a lower amount of lamellae in P-2. In addition, both DSC and SAXS results suggested that the amount of fibrils in P-2 is larger than in P-1 whereas the amount of lamellae is greater in P-1 than in P-2. Finally, at large DR, the DSC and SAXS data implied that the most parts of crystals have formed a fibrillar structure, although some lamellae may be still present.

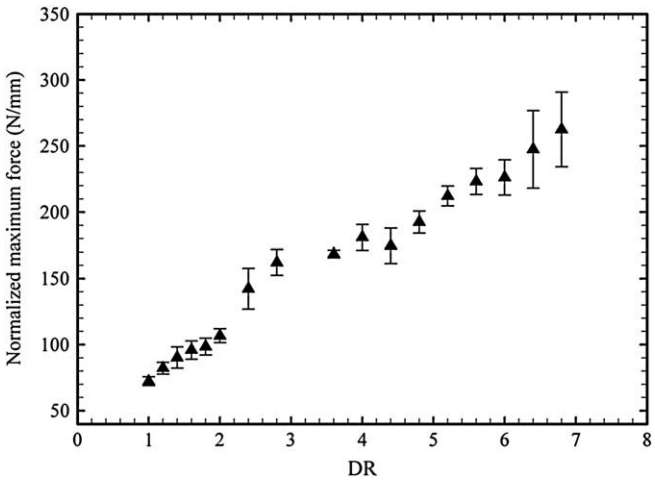

Fig. 12. Normalized maximum force for piercing as a function of draw ratio for P-1.

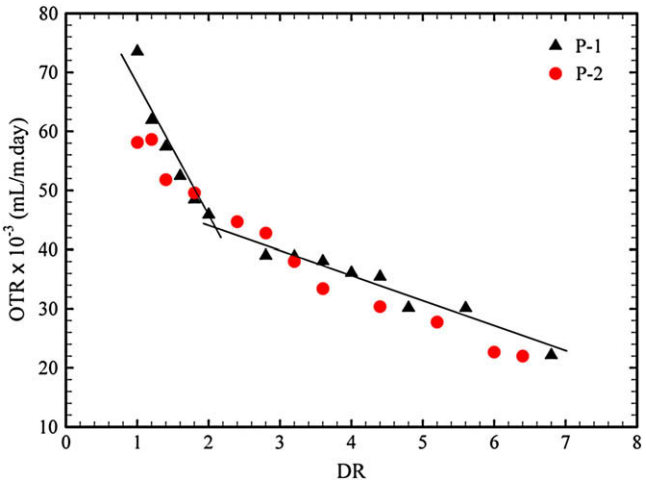

Fig. 13. Normalized oxygen transmission rate (OTR) as a function of draw ratio for P-1 and P-2.

The mechanical and tear behaviors are closely related to structure changes [24] as seen in Fig. 11 that reports the tear resistance of the films along MD. A remarkable reduction in tear occurs when DR varies from 1 to 2.8 while further increasing DR hardly affects the tear resistance: the higher the orientation of the crystalline and amorphous phases, the lower the tear resistance along MD. At low DR, P-1 shows slightly lower tear resistance than P-2, which is due to its better orientation. Measurements of the tear resistance along TD for samples stretched beyond DR = 2.4 were not possible, because the tearing direction deviated most of the time to MD. In fact, there was a high resistance in TD when compared to MD, which caused a crack in MD and created errors and non-reproducible data that are not reported here. This implies and confirms that by increasing DR a fibrillar structure with fibrils aligned in MD is formed.

Sadeghi et al. [1] reported significant increases of the Young modulus, yield stress, tensile strength along MD and a drastic decrease in elongation at break along TD for uniaxial drawn polypropylene films. In this study, puncture tests were performed to investigate the effects of MDO stretching on the mechanical properties of the samples along ND and the results are presented in Fig. 12. Each point is an average over 10 samples. A linear dependence of the maximum piercing force as a function of DR is observed. As pointed out earlier, increasing DR enhances the

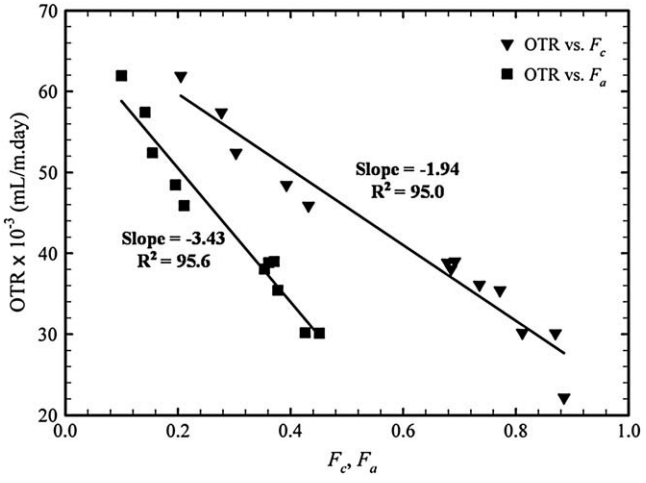

Fig. 14. Normalized oxygen transmission rate (OTR) as a function of crystalline, F_c, and amorphous, F_a, orientation functions.

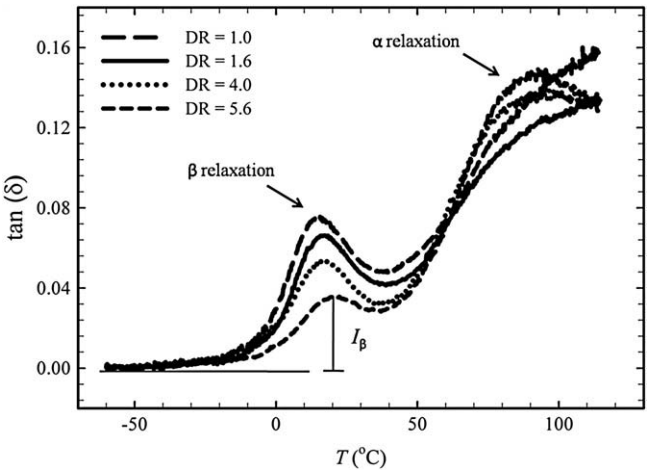

Fig. 15. DMTA-tan (δ) as a function of temperature for P-1 at different DRs.

crystallinity, the crystal thickness as well as the alignment of the crystalline and amorphous phases (see Figs. 2–4). Since the crystalline phase is stronger and stiffer than the amorphous phase [25], these can explain the improvement of the puncture resistance with increasing DR.

Another application for MDO stretched films is the reduction of gas permeability or improvement of barrier properties. In the literature [26–28], controversies regarding the interpretations for the relationship between the structural parameters of polymeric films in particular PP and their gas permeability could be found. According to Taraiya et al. [26], the key factor that controlled the permeation of gas molecules through the oriented PP films was the orientation of the amorphous phase, although they did not present sufficient data to support this idea. In recent studies [27,28], low gas permeability in biaxially oriented polypropylene (BOPP) films was attributed to the decrease in chain motions in the amorphous phase.

Fig. 13 reports the oxygen transmission rate (OTR) normalized (multiplied) by the films thickness as a function of DR for P-1 and P-2. OTR is reduced by around 75% when DR increases to 7.2. However, it should be noticed that an appreciable decrease in OTR is seen in the DR range of 1–2.4 and the trends for both P-1 and P-2 are somewhat the same. The similarity of the DR dependence of the oxygen transmission rate (Fig. 13) and orientation functions (Figs. 3 and 4) suggested a correlation between both set of data. Fig. 14 presents the normalized OTR values as a function of the crystalline, F_c, as well as the amorphous, F_a, orientation functions for P-1. Reasonable linear correlations between the orientation parameters and OTR are observed: the higher the orientation of crystalline and amorphous phases, the lower the oxygen permeability. It is important to note that OTR has a stronger dependence on F_a than on F_c (the slope of the least-squares regression fit is −3.43 for the former and −1.94 for the latter). This suggests that the orientation of the amorphous phase has more impact on the drop in oxygen permeability compared to the orientation of the crystalline phase. A similar behavior for the P-2 films was observed (not shown). It is well understood that the crystalline part of semi-crystalline polymers is impermeable to gas transport. In other words, the gas diffusion occurs only through the amorphous region. This is in agreement with the interpretation mentioned above about the amorphous phase role in OTR reduction.

In the MDO process, the crystals are aligned into MD and this not only enhances the orientation of the phases but also increases the tautness of tie chains and hence reduces the amorphous chains mobility [27]. In PP, the main chain motion in the amorphous phase can be characterized through the dynamic mechanical β-relaxation peak [27] as obtained from the dynamic mechanical thermal response of Fig. 15 (tan δ as a function of temperature, in the range from −60 °C to 115 °C) for P-1 films at four DR values. The first peak at about 10 °C is attributed to the β-relaxation whereas the second peak at about 100 °C to the α-relaxation. Obviously, increasing DR has a major impact on the β-relaxation peak whereas the α-relaxation remains almost unchanged. Following Lin et al. [27,28], the OTR data are plotted in Fig. 16 versus the β-relaxation intensity, I_β, as determined from the peak magnitude of the DMTA-tan δ curves of Fig. 15. Good linear correlations between the oxygen transmission rate and β-relaxation intensity for P-1 and P-2 are observed, confirming the findings of Lin et al. [28] for biaxially oriented polypropylene (BOPP) films. Limited amorphous tie chains mobility (low I_β) leads to a low oxygen transmission, and inversely, a high amorphous tie chains motion (high I_β) results in a high oxygen permeability. However, it is clear that the data for P-1 and P-2 do not coincide, in contrast to the results of Lin et al. [28] that were independent of the resin type and thermal history. In summary, the improvement of barrier properties with increasing DR could be explained by the enhancement of the crystalline and amorphous phase orientation, but also by the reduction of the amorphous tie chains mobility.

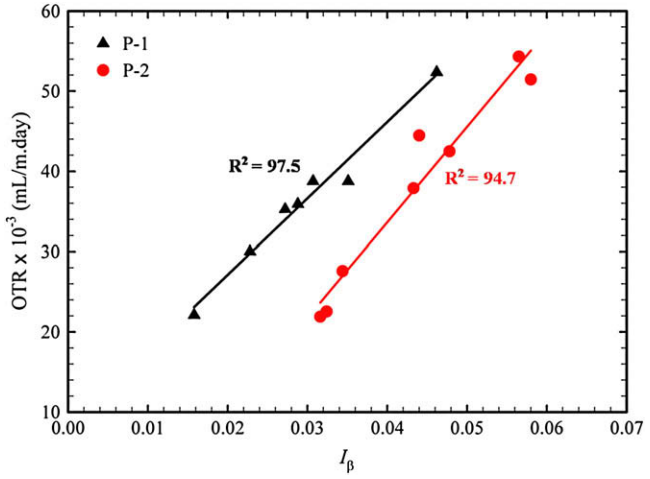

Fig. 16. Normalized oxygen transmission rate as a function of the β-relaxation intensity for P-1 and P-2.

4. Conclusions

In this work, precursor films with coexisting rows of lamellae and spherulites and only spherulites were produced and then uniaxially hot stretched using a machine direction orientation (MDO) unit. Changes in morphology in relation with the barrier properties as well as tear and puncture properties are presented. Our findings can be summarized as follows:

- MDO stretching caused a morphological transformation of the spherulites into fibrils at high DR, yielding thicker crystals and, subsequently, a higher melting point.
- Compared to films obtained from precursor films of coexisting rows of lamellae and spherulites (P-1), drawn films made from precursor films of only a spherulitic structure (P-2) showed a lower crystal orientation at low DR, but a better crystal alignment at high DR. This was explained by the larger size of the PP spherulites compared to the small rows of lamellae, resulting in a better deformation of the spherulites.

- Increasing DR significantly increased the puncture resistance along ND and drastically decreased the tear resistance along MD. These were attributed to the thicker crystal size and higher orientation of the fibrils compared to the random rows of lamellae and/or spherulites.
- Linear correlations between the oxygen transmission rate (OTR) and crystalline as well as amorphous orientation functions (F_c and F_a, respectively) were found.
- OTR was also linearly correlated with the chain mobility in the amorphous part. The higher the amorphous tie chain mobility, the higher the OTR.

Acknowledgements

Financial support from NSERC (Natural Science and Engineering Research Council of Canada) is gratefully acknowledged. We also acknowledge the large infrastructure grant received from the Canadian Foundation for Innovation (Governments of Canada and Province of Quebec), which allowed us to build the unique POLYNOV facility. We are also thankful to Messrs. P. Cigana, L. Parent and P.M. Simard for their technical help. Finally, we are thankful to ExxonMobil for donating the resin used in this work.

References

[1] Sadeghi F, Carreau PJ. Can Chem Eng J 2008;86:1103–10.
[2] Schut JH. Plastics Technol 2005;51:48–51.
[3] McGonigle EA, Liggat JJ, Pethrick RA, Jenkins SD, Daly JH, Hayward D. Polymer 2001;42:2413–26.
[4] Backman A, Lange J, Hedenqvist MS. J Polym Sci Part B Polym Phys 2004;42:947–55.
[5] Dias P, Lin YJ, Hiltner A, Baer E, Chen HY, Chum SP. J Appl Polym Sci 2008;107:1730–6.
[6] Srinivas S, Brant P, Huang Y, Paul DR. Polym Eng Sci 2003;43:831–49.
[7] Gould RJ. Polym Eng Sci 1988;28:857–61.
[8] Tabatabaei SH, Carreau PJ, Ajji A. J Membr Sci 2008;325:772–82.
[9] Sadeghi F, Ajji A, Carreau PJ. J Membr Sci 2007;292:62–71.
[10] Nie HY, Walzak MJ, McIntyre NS. Polymer 2000;41:2213–8.
[11] Diez J, Alvarino C, Lopez J, Ramirez C, Abad MJ, Canol J, et al. J Therm Anal Cal 2005;81:21–5.
[12] Zuo F, Keum JK, Chen X, Hsiao BS, Chen H, Lai SY, et al. Polymer 2007;48:6867–80.
[13] Sakurai T, Nozue Y, Kasahara T, Mizunuma K, Tamaguchi N, Tashiro K, et al. Polymer 2005;46:8846–58.
[14] Fujiyama M, Inata H. J Appl Polym Sci 2002;84:2157–70.
[15] Tabatabaei SH, Carreau PJ, Ajji A. Polymer, in press.
[16] Arroyo M, Lopez-Manchado MA. Polymer 1997;38:5587–93.
[17] Sadeghi F, Ajji A, Carreau PJ. Polym Eng Sci 2007;47:1170–8.
[18] Cole KC, Ajji A. Orientation characterization in polypropylene. In: Karger-Kocsis J, editor. Polypropylene an A–Z reference. Dordrecht, The Netherlands: Kluwer Academic Publishers; 1999.
[19] Alexander LE. X-ray diffraction methods in polymer science. New York: Wiley Inter Science; 1969.
[20] Somani RH, Yang L, Zhu L, Hsiao BS. Polymer 2005;46:8587–623.
[21] Elias MB, Machado R, Canevarolo SV. J Therm Anal Cal 2000;59:143–55.
[22] Ajji A, Zhang X, Elkoun S. Polymer 2005;46:3838–46.
[23] Zhang X, Ajji A. Polymer 2005;46:3385–93.
[24] Zhang XM, Elkoun S, Ajji A, Huneault MA. Polymer 2004;45:217–29.
[25] Strawhecker KE, Manias E. Macromolecules 2001;34:8475–82.
[26] Taraiya AK, Orchard GAJ, Ward IM. J Polym Sci Part B Polym Phys 1993;31:641–5.
[27] Lin YJ, Dias P, Chen HY, Chum S, Hiltner A, Baer E. Polym Eng Sci 2008;48:642–8.
[28] Lin YJ, Dias P, Chen HY, Chum S, Hiltner A, Baer E. Polymer 2008;49:2578–86.